Generating a 3D H3 potential energy surface from the 1D surface

Noam Agmon

Citation: The Journal of Chemical Physics **76**, 743 (1982); doi: 10.1063/1.442685
View online: http://dx.doi.org/10.1063/1.442685
View Table of Contents: http://scitation.aip.org/content/aip/journal/jcp/76/1?ver=pdfcov
Published by the AIP Publishing

e product neutrals from the metal ions as is observed ere.

In the gas phase, binary reaction of N_2O_5 with NO has ot been observed.[4] The direct reaction of NO with $_2O_5$ to form N_2O_4 is slightly exothermic,[5] $-\Delta H^\circ_{298}(4)$ 14.2 kcal mol^{-1}. It would seem that the most plausible nechanism to account for the larger reactivity of the lkali ion clustered N_2O_5 with NO involves O atom abstraction from one of the nitro groups in N_2O_5 leaving an $ONO-NO_2$ molecule clustered to X^+. However, the stable form of N_2O_4 is O_2N-NO_2 so that the above mechanism that forms $ONO-NO_2$ is less exothermic unless O_2N-NO_2 is formed by rearrangement during the collision. In any case, not enough energy is released in the reaction to dissociate the N_2O_4 product from the alkali ion, and, in fact, the N_2O_4 is observed to remain clustered to Li^+ and Na^+. It is possible that the ions denoted as $X^+ \cdot N_2O_4$ may actually be $X^+ \cdot 2NO_2$. Since the reaction of NO and N_2O_5 to produce three NO_2 molecules is thermoneutral, this possibility remains as long as the bond energy of two NO_2 molecules clustered to X^+ is greater than that of one N_2O_5 molecule.

It is possible to envision the clusters $X^+ \cdot N_2O_5$ as $NO_2^+ \cdot XNO_3$ provided the bond dissociation energies of $X-NO_3$ are sufficiently large. Unfortunately, the thermochemical values needed to deduce the bond dissociation energies for $Na-NO_3$ and $Li-NO_3$ are not known. However, support for the identification $X^+ \cdot N_2O_5$ is obtained experimentally from our observation that H_2O rapidly reacts to displace N_2O_5 from $X^+ \cdot N_2O_5$.

Finally, the neutral–neutral reactions [Reactions (6) and (8)] are also extremely slow.[7,8] The very large activation barrier for these reactions is not overcome when one of the reactant neutrals is clustered to an ion; i.e., Reactions (5) and (7).

In the cases studied in these measurements, the presence of the catalytic ion lowers the activation energy for the neutrals involved. This conclusion is drawn from the magnitude and temperature dependences observed for the reactions reported here. The rate constants for ion clustered O_3 and N_2O_5 with NO are many orders of magnitude greater than the rate constants for the reactions of these neutrals with NO in the absence of the catalytic ion. Also, no temperature dependence is observed for the ion catalyzed reactions while an activation energy of 2.9 kcal mol^{-1} was measured for the reaction of O_3 with NO and a much larger barrier must exist for the reaction of N_2O_5 with NO.

From the data presented in Table I, it seems clear that there is a strong inverse relation between the enhanced reactivity of the clustered neutral with NO and the radius of the alkali metal ion which is 0.60, 0.95, and 1.33 Å for Li^+, Na^+, and K^+, respectively.[6] Several mechanisms can be visualized to explain the enhancement of the clustered neutral reactions with NO and all would suggest such a correlation.[4]

The reactivity of neutral molecules is observed to be greatly enhanced in several cases when one of the neutrals is clustered to an ion which does not participate directly in the reaction. The rate constants appear to be most enhanced when the neutrals are clustered to alkali metal ions of low atomic weight. No temperature dependence is observed for these ion catalyzed reactions.

This research was supported in part by the Defense Nuclear Agency.

[a]Centre National de la Recherche, Scientifique Laboratories d'Aerothermique, 4 ter des Gardes, 92190 Meudon, France.
[b]Max-Plank-Institut für Kernphysik, Postfach 1039 80, D-6900 Heidelberg I, West Germany.
[c]Cooperative Institute for Research in Environmental Science (CIRES) Fellow.
[d]NOAA National Research Council Postdoctoral Research Associate, 1979–1980.

[1]R. A. Perry, B. R. Rowe, A. A. Viggiano, D. L. Albritton, E. E. Ferguson, and F. C. Fehsenfeld, Geophys. Res. Lett. 7, 693 (1980).
[2]E. E. Ferguson, F. C. Fehsenfeld, and A. L. Schmeltekopf, Adv. At. Mol. Phys. 5, 1 (1969).
[3]J. W. Birks, B. Shoemaker, T. J. Leck, and D. M. Hinton, J. Chem. Phys. 65, 5181 (1976).
[4]A. A. Viggiano, Thesis, Department of Chemistry, University of Colorado, 1980; A. A. Viggiano, J. A. Davidson, F. C. Fehsenfeld, and E. E. Ferguson, J. Chem. Phys. 74, 6113 (1981).
[5]D. R. Stull and H. Prophet, JANAF Thermochemical Tables, 2nd ed., Natl. Stand. Ref. Data Ser., Natl. Bur. Stand. 37 (U.S. GPO, Washington, D.C., 1971).
[6]K. G. Spears, J. Chem. Phys. 57, 1842 (1972).
[7]L. M. Arin and P. Warneck, J. Chem. Phys. 76, 1514 (1972).
[8]D. L. Dawbendick and J. G. Calvert, Environ. Lett. 8, 103 (1975).

Generating a 3*D* H_3 potential energy surface from the 1*D* surface

Noam Agmon[a]

Department of Physical Chemistry, The Hebrew University, Jerusalem, Israel
(Received 17 November 1980; accepted 28 January 1981)

The knowledge of the potential energy surface (PES) for a polyatomic system is essential for dynamical calculations.[1] In spite of this, only H_3 has been calculated *ab initio* to "chemical accuracy" of 1 kcal/mol.[2] Thus, while *ab initio* methods retain their central position as an absolute reference for comparison, semi-

 0021-9606/82/010743-03$02.10

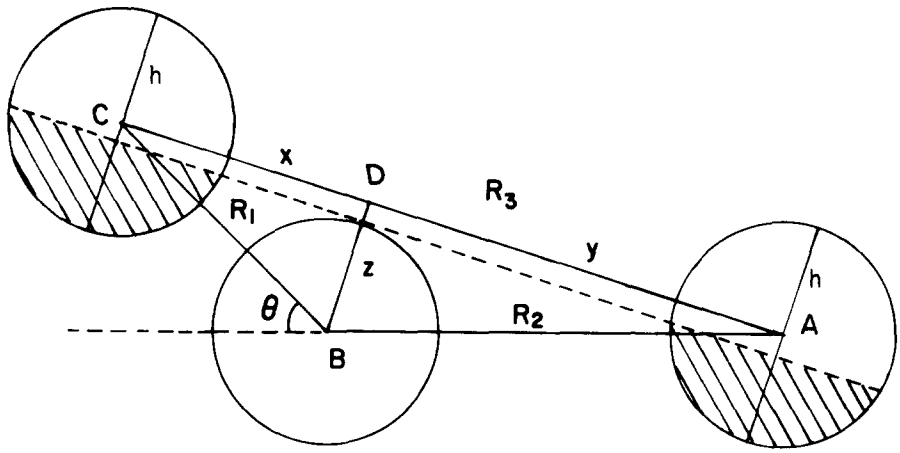

FIG. 1. Three identical spheres at distances R_i and an angle θ. The shadowed regions are those screened by the central sphere.

empirical methods are developed[1] with a twofold aim: A better understanding of the topology of the surface, and a simple procedure for its generation.

We have previously[3] presented an analysis of collinear ($1D$) triatomic PES, where the three atoms (denoted by A, B, and C) are confined to a straight line. On curves parallel to the reaction coordinate (the "bond order coordinates") one has "reduced" profiles of the energy along the reaction coordinate. On the curves perpendicular to the bond order coordinates, one has reduced Morse curves related to the reagent's and product's diatomic curves.

We now consider the three dimensional ($3D$) PES, which is a function, not only of the two bond distances $R_1 \equiv R_{BC}$ and $R_2 \equiv R_{AB}$, but also of the angle θ, as defined in Fig. 1. We wish to rationalize the qualitative trend observed for the H_3 system,[2] namely, an increase in θ shifts the barrier's location ($R_1^{\ddagger}$, $R_2^{\ddagger}$) to larger nuclear separations, and increases its height.

In the H_3 system, the spin of each end atom (A or C) is paired with that of the central atom B. Hence the spins of A and C are expected to be unpaired, leading to a triplet interaction between them.[4] At first sight it seems that one may explain the above trend as following from this interaction: For given R_1 and R_2, the larger θ (up to an angle of 120°) the smaller $R_3 \equiv R_{AC}$, hence the larger the triplet interaction. However, when one simply adds the H_3 triplet function[5] $V^*(R_3)$ to the collinear PES, $V(R_1, R_2, \theta = 0)$, it is found that the shift in location, and increase in height of the barrier with θ is too drastic. Hence, there must be an additional effect, which we call a "classical screening" effect.

Let us picture the three H atoms as charged spheres, where, as in classical electrostatics, the charge is

TABLE I. A comparison of Eq. (1) with exact computation[a], (energies are relative to dissociation). $h = z$ is given by Eq. (4), with H atom diameter $d = 2$ a.u. $V^*(R)$ is the $b\,^3\Sigma_u^+$ curve[b] as fitted by Eq. (5). $V(R_1, R_2, \theta = 0)$ is the collinear H_3 PES given in Ref. 3, with a ground state H_2 curve taken from a fit (Ref. 9) to the exact curve.[b] The H_2 parameters were slightly modified to suit those of Ref. 2, namely, $R_e = 1.4014$ a.u. and $D_e = 173.7$ mhartree (1 mhartree $= 10^{-3}$ a.u. $= 0.628$ kcal/mol). The parameters used in the collinear potential chosen to reproduce the barrier's location and height are Pauling's parameter $a = 0.5139$ a.u., the barrier's height $V_b^0 = 15.6$ mhartree. The equipotential contours (Ref. 10) are not shown, but they are similar to Fig. 2 in Ref. 8. The complete table is available upon request.

$\theta = 30°$				$\theta = 60°$				$\theta = 90°$			
R_1 (a.u.)	R_2 (a.u.)	$-V$, Ref. 2 (mhartree)	$-V$, Eq. 1 (mhartree)	R_1 (a.u.)	R_2 (a.u.)	$-V$, Ref. 2 (mhartree)	$-V$, Eq. 1 (mhartree)	R_1 (a.u.)	R_2 (a.u.)	$-V$, Ref. 2 (mhartree)	$-V$, Eq. 1 (mhartree)
1.17	1.170	47.3	16.8	1.20	1.200	47.8	19.2	1.500	1.500	102.7	97.4
1.37	1.370	117.7	109.0	1.40	1.400	112.2	104.2	1.700	1.700	121.8	122.3
1.57	1.570	147.9	145.5	1.60	1.600	139.9	138.7	1.800	1.800	125.1	127.0
1.67	1.670	153.7	152.5	1.70	1.700	145.3	145.4	1.900	1.900	125.4	128.3
1.77	1.770	155.3	154.7	1.80	1.800	146.8	147.7	2.000	2.000	123.5	127.1
1.87	1.870	153.8	153.5	1.90	1.900	145.4	146.8	2.100	2.100	120.0	124.0
1.97	1.970	149.9	149.9	2.00	2.000	141.9	143.5	2.300	2.300	109.5	114.1
2.17	2.170	137.6	137.9	2.20	2.200	130.3	132.3	2.500	2.500	96.6	101.7
2.47	2.470	113.4	114.6	2.50	2.500	107.5	110.2	1.400	1.200	54.5	34.0
2.67	2.670	96.5	98.6	1.40	1.000	25.1	−3.6	1.780	1.580	121.8	121.3
1.40	1.000	37.4	12.5	1.66	1.142	97.7	90.1	1.920	1.720	126.8	128.3
1.56	1.100	89.6	79.3	1.74	1.276	125.0	121.7	1.990	1.790	127.0	129.3
1.65	1.245	125.7	121.1	1.82	1.409	140.0	139.1	2.060	1.860	126.1	128.9
1.74	1.380	144.5	142.5	1.90	1.543	146.9	147.2	2.200	2.000	121.7	125.2
1.83	1.515	153.5	152.7	1.94	1.610	148.2	148.8	2.340	2.140	114.7	118.7
1.92	1.650	155.9	155.5	1.98	1.677	148.3	149.2	1.780	1.110	80.2	69.7
2.01	1.785	153.8	153.7	2.02	1.743	147.4	148.6	2.020	1.450	130.4	128.3
2.10	1.920	148.6	148.7	2.14	1.944	140.9	142.5	2.140	1.620	134.2	134.1
2.01	0.970	77.8	77.0	1.88	1.032	85.1	80.7	2.260	1.790	131.1	132.4
2.09	1.250	145.2	145.9	1.94	1.164	120.0	118.3	2.500	2.130	114.2	117.3

[a]Reference 2.

[b]Reference 5.

mogeneously spread on their outer envelopes. In e interaction between A and C, the influence of B is ; in an eclipse—it simply "casts its shadow" on A r on C). The shadowed area of A (or of C, the two re identical in the case of H_3) is screened. Only the nscreened dome of A interacts with C. The fraction f this nonscreened area is h/d, where d is A's diameter and h is the dome's height. Hence the $3D$ PES is ;iven by

$$V(R_1,\ R_2,\ \theta) = V(R_1,\ R_2,\ \theta=0) + V^*(R_3)h/d\ . \tag{1}$$

The height of the unscreened dome h is easy to calculate. From Fig. 1 it is evident that $h = z \equiv \overline{BD}$. Define $x \equiv \overline{CD}$ and $y \equiv \overline{AD}$ as in the figure. Then,

$$x^2 + z^2 = R_1^2\ ,\quad y^2 + z^2 = R_2^2\ , \tag{2}$$

$$x + y = R_3 = (R_1^2 + R_2^2 + 2R_1R_2\cos\theta)^{1/2}\ . \tag{3}$$

These equations are solved for z as follows:

$$z = [R_1^2 - (R_3^2 + R_1^2 - R_2^2)^2/4R_3^2]^{1/2}\ . \tag{4}$$

For a collinear configuration ($R_3 = R_1 + R_2$) one finds from Eq. (4) that $z = 0$, hence A is completely screened by B. This condition is necessary for Eq. (1) to be consistent.

For the purpose of computation, we have fitted the H_2 triplet function, $b\,^3\Sigma_u^+$,[5] to an "anti-Rydberg"[6] potential of the form

$$V^*(R) = (A - BR)\exp(-\alpha R)\ , \tag{5}$$

with $A = 1.399$ a.u., $B = 0.1447$ a.u., and $\alpha = 1.200$ a.u. Equation (5) has the property that if one defines[7] $n \equiv \exp(-\alpha R)$, $V^*(n) = An + (B/\alpha)n\ln n$ is a one bond order (n) analog of the energy profile[3] along the reaction coordinate.

A computational procedure for checking the above model is to take the best fit[8] to the exact collinear H_3 PES[2] for $V(R_1,\ R_2,\ \theta = 0)$. Here, however, we choose to show how our empirical collinear PES[3] generalizes to $3D$. This PES is "chemically accurate" for most low energy configurations but deteriorates at high energies, especially at the "repulsive wall" (small R_i's).

Table I shows a comparison with all *ab initio* points[2] for $\theta = 30°$, $60°$, and $90°$. The agreement is surprisingly good for such a simplistic model. This agreement deteriorates at high energies (partly due to our collinear function) and for large θ. Indeed, a model which treats the three H–H pairs in a nonsymmetric fashion is not expected to give good results for $\theta \to 120°$.

The problem of using the present method for other triatomics is partly the generalization of the "screening function" to nonidentical atoms, and mainly the identification of the interaction between the end atoms.

[a]Present address: Department of Chemistry, California Institute of Technology, Pasadena, CA 91125.

[1]R. D. Levine and R. B. Bernstein, *Molecular Reaction Dynamics* (Oxford University, New York, 1974); *Atom–Molecule Collision—A Guide to the Experimentalist*, edited by R. B. Bernstein (Plenum, New York, 1979).
[2]B. Liu, J. Chem. Phys. **58**, 1925 (1973); P. Siegbahn and B. Liu, *ibid.* **68**, 2457 (1978).
[3]N. Agmon and R. D. Levine, J. Chem. Phys. **71**, 3034 (1979).
[4]For example, see, A. A. Zavitsas, J. Am. Chem. Soc. **94**, 2779 (1972); H. S. Johnston, *Gas Phase Reaction Rate Theory* (Ronald, New York, 1966), p. 180.
[5]W. Kołos and L. Wolniewicz, J. Chem. Phys. **43**, 2429 (1965).
[6]R. Rydberg, Z. Phys. **73**, 376 (1931); **80**, 514 (1933).
[7]L. Pauling, J. Am. Chem. Soc. **69**, 542 (1947).
[8]D. G. Truhlar and C. J. Horowitz, J. Chem. Phys. **68**, 2466 (1978) **71**, 1514 (E) (1979).
[9]O. Kafri, Chem. Phys. Lett. **61**, 538 (1979).
[10]N. Agmon, Ph. D. thesis, The Hebrew University of Jerusalem, 1980.

The emission spectrum from gaseous HCl^+ produced by photoionization

Bilin P. Tsai and Lynda L. Parrella

Department of Chemistry, University of Minnesota, Duluth, Minnesota 55812
(Received 10 July 1981; accepted 8 September 1981)

The emission spectrum of HCl^+ was first observed[1] after passing gaseous HCl through an electrical discharge; it was assigned to the $A\,^2\Sigma^+ \to X\,^2\Pi_i$ transitions of the molecular ion. Similar experiments[2–5] revealed the $A\,^2\Sigma^+(v' = 0–6) \to X\,^2\Pi_i(v'' = 0)$ vibrational and rotational bands. The first observation of HCl^+ emission following collision with a single particle was reported by Haugh[6] in 1972. In this study, the radiative bands resulted after collision with He^*. In 1973, the $A \to X$ optical spectrum following Penning ionization was reported.[7]

Similarities in the electron energy distributions following photoionization[8] and Penning ionization[9] of HCl indicate that vertical transitions occur in both excitation processes. However, emission spectra show that higher vibrational states produced by collisions with metastable[7] or ionic[6] helium are depopulated prior to radiative decay.

This investigation is the first report of the emission spectrum of photoionized HCl^+. We report strong $A\,^2\Sigma^+(v' = 0–6) \to X\,^2\Pi_i(v'' = 0)$ transitions and weaker bands assigned to $A\,^2\Sigma^+(v' = 1–3) \to X\,^2\Pi_i(v'' = 1)$. The analysis of these bands yields electronic state separation and vibrational frequency values which are in agree-

 0021-9606/82/010745-03$02.10